Analyst

PAPER

View Article Online
View Journal | View Issue

Cite this: *Analyst*, 2015, **140**, 1974

Aminolevulinic acid with gold nanoparticles: a novel theranostic agent for atherosclerosis

Karina de Oliveira Gonçalves,[a] Monica Nascimento da Silva,[a] Letícia Bonfante Sicchieri,[b] Flávia Rodrigues de Oliveira Silva,[c] Ricardo Almeida de Matos[a] and Lilia Coronato Courrol*[a,b]

Received 24th November 2014,
Accepted 31st January 2015

DOI: 10.1039/c4an02166e

www.rsc.org/analyst

In this study, 5-aminolevulinic acid (ALA) gold nanoparticles (ALA:AuNPs) functionalized with polyethylene glycol (PEG) were synthesized and administered to rabbits to evaluate their use in clinical practice as theranostic agents for atherosclerosis. This was done by measuring the porphyrin fluorescence extracted from the rabbits' blood and feces. An increase in blood and feces porphyrin emission after ALA:AuNP administration suggests that ALA was incorporated by gold nanoparticles, its structure was preserved, and a rapid conversion into endogenous porphyrins occurred, overloading the synthetic pathway that led to protoporphyrin IX (PPIX) accumulation. This finding indicated that this method can aid in the early diagnosis and therapy of atherosclerosis with high sensitivity.

A. Introduction

Atherosclerosis, or hardening of the arteries, is the main cause of heart attacks, strokes, and peripheral vascular diseases. It is characterized by endothelial cell injury, lipoprotein deposition, inflammation reaction, cell proliferation, vascular remodeling, plaque formation and expansion and rupture, culminating in thrombosis of the vessel.[1]

Atherosclerotic cardiovascular disease and cancer are the leading causes of death in the world. Atherogenesis and neoplasia have some common points such as oxidative stress and cellular damage that results from angiogenesis, and the accumulation of protoporphyrin IX.[2] The shared features of atherosclerosis and cancer justify similar novel approaches to diagnosis and therapy.

The theranostic agents are capable of providing both a diagnostic as well as a therapeutic function.[3] A significant growth in the field of theranostics for cancer and inflammatory diseases, such as atherosclerosis, has occurred in the last decade.[4,5] Although light-mediated theranostics are selective they cause significant tissue damage and induce inflammatory reactions, which can lead to disease recurrence.[6]

Gold nanoparticles (AuNPs) are emerging as promising agents for cancer and atherosclerosis theranostics.[3,4] Gold nanoparticles exhibit unique physicochemical properties including surface plasmon resonance effect, good light scattering, absorption capability, small size, high atomic number, biocompatibility and the ability to bind targeting agents, implying that they have potential as contrast agents.[5] In addition, the combination of AuNPs and diffusion reflection[6] (DR) presents a method to detect cancer and atherosclerosis at its early stages.[7] The unique surface plasmon resonance feature of AuNPs makes them candidate materials for photothermal therapy (PTT).[8] AuNPs can act as energy transducers, converting light into heat and causing selective macrophage depletion.[8] Compared with conventional drug delivery, such a treatment is active only within the limited illumination area, therefore minimizing normal tissue damage.[7]

The use of gold nanoparticles as carriers of photosensitizers is a very promising approach for photodynamic therapy (PDT), a noninvasive treatment modality for atherosclerosis and cancers.[8] PDT involves the administration of photosensitizer (PS) molecules that bind to the atherosclerosis plaques[9] (or cancerous cells), and subsequently, under irradiation with appropriate light, produce reactive oxygen species (ROS) that chemically destroy the plaques. 5-Aminolevulinic acid (ALA)-based PDT is gaining increasing attention in medicine.[10] The external addition of ALA results in enhanced synthesis of protoporphyrin IX (PPIX) by the cellular heme biosynthetic pathway. PDT mediated by ALA has low dark toxicity to cells, rapid clearance from the body (24–48 h) and rapid conversion

[a]*Universidade Federal de São Paulo, Laboratório de Lasers e Óptica Biomédica Aplicada (LOBA) Instituto de Ciências Ambientais, Químicas e Farmacêuticas (ICAQF), Departamento de Ciências Exatas e da Terra (DCET), Rua Artur Riedel, 275 Eldorado, 09972-270 – Diadema, SP, Brazil. E-mail: lccourrol@gmail.com; Fax: +551140436428*
[b]*Instituto de Pesquisas Energéticas e Nucleares, Centro de Lasers e Aplicações, São Paulo, SP, Brazil*
[c]*Instituto de Pesquisas Energéticas e Nucleares, Centro de Ciência e Tecnologia de Materias, São Paulo, SP, Brazil*

into PPIX through the heme cycle.[15] It was demonstrated that ALA-derived PPIX preferentially accumulates in atherosclerotic plaques, and its fluorescence intensity is positively correlated with the plaque macrophage content.[8] The use of AuNPs as vehicles for 5-ALA delivery represents a promising approach, especially with the recent demonstration that the immobilization of PS on the particle surface is better for ROS formation.[11,12]

Another possible therapeutic use of ALA is in sonodynamic therapy,[13,14] which realized the strategy of reducing the infiltration of macrophages in atherosclerotic plaques, and might be a good treatment for atherosclerosis.[15]

In this study, ALA gold nanoparticles (ALA:AuNPs) functionalized with polyethylene glycol (PEG) were synthesized and administered to rabbits to evaluate their use in clinical practice as theranostic agents for atherosclerosis. This was done by measuring the PPIX fluorescence extracted from the rabbits' blood and feces.

Table 1 Experimental groups

Groups	Characteristics
CG – Control group	4 animals Normal diet
EG – Experimental group	3 animals Diet containing 1% cholesterol (Sigma-Aldrich)
CGALA – Control group and ALA	3 animals Normal diet and oral ALA administration
EGALA – Experimental group and ALA	3 animals Diet containing 1% cholesterol (Sigma-Aldrich) diluted in chloroform and oral ALA administration
EGALAAu – Experimental group and ALA:AuNPs	3 animals Diet containing 1% cholesterol (Sigma-Aldrich) diluted in chloroform and oral ALA:AuNP administration

B. Materials and methods

ALA:AuNP solution

Tetrachloroauric acid ($HAuCl_4$) and 5-aminolevulinic acid hydrochloride ~98% (A3785) were purchased from Sigma-Aldrich. To prepare ALA gold nanoparticle (ALA:AuNP) solutions, ~21 mg of $HAuCl_4$ were mixed with ~83 mg of ALA in 200 mL of distilled water at 20 °C. The process was accompanied by vigorous stirring for 5 minutes, and the resulting solution was exposed to a 150 watt xenon lamp for 2 minutes.

The solutions' UV-Vis absorption spectra were measured by using a Varian Cary 17D spectrophotometer, using 1 cm quartz cells.

Transmission electron micrographs were obtained from a Jeol (Zeiss, Germany) transmission electron microscope (TEM), with images captured using a MegaView III camera and processed with the software ITEM (Universal TEM Imaging Platform (Olympus Soft Imaging Solutions GmbH, Germany)). For this, a drop of gold nanoparticles dispersed in distilled water was placed onto a carbon-coated copper grid, the excess liquid was removed using a paper wick, and the deposit was dried in air prior to imaging.

Animal experimentation

A total of 16 adult white male rabbits (New Zealand species *Oryctolagus cuniculus*, weighing 2.3 ± 0.1 kg, and ~3.5 months of age) were divided into the groups as shown in Table 1.

The animals were individually housed in a controlled environment that was maintained at 19 °C; food and water were provided *ad libitum*. Blood samples were extracted in the beginning and after 34 days and 60 days, and feces samples were collected after 33 days. After 60 days, the animals were anesthetized by an injection of ketamine and xylazine and then euthanized by a heart injection of 1 mL of potassium chloride, according to the American Veterinary Medical Association guidelines for euthanasia.

The Ethics Committee of UNIFESP approved the protocol of this study (CEUA no. 1147091113).

Biochemical analyses of blood serum

After overnight fasting, blood was drawn from the marginal ear vein at the baseline time point. The blood samples were stored on ice for 2 h and centrifuged (3000 rpm, 10 min, 4 °C) to obtain serum. The total cholesterol (TC), high-density lipoprotein HDL-C, low-density cholesterol (LDL-C) and glucose levels in the serum samples were assessed using an enzymatic colorimetric assay (Labtest Diagnostic S.A) with an automatic biochemical analyzer.

Porphyrin extraction

Three parts by volume of analytical grade acetone were added to one part of the total blood or macerated feces, and the resulting combination was mixed well. This mixture was centrifuged at 4000 rpm for 15 min. The clear supernatant of the mixture was stored in a clean tube, and spectrofluorimetric analyses were performed on the same day.

Administration of ALA solution

Solutions of ALA were freshly prepared at a concentration of 60 mg kg^{-1} and 100 mg mL^{-1} in physiological serum. The pH of the solutions was adjusted to 6.8 using NaOH.

The ALA:AuNPs were prepared in a concentration of ~57.74 mg kg^{-1}. ALA and ALA:AuNPs were orally administered to the animals with syringes (~3.75 mL).

Blood was collected before and ~4 hours after ALA and ALAAu administration, and also before and 34 and 60 days after introduction of the diet procedure.

Artery excision and histological analysis

The rabbits' arteries were excised and washed in PBS. Cryosections of the aortic arch specimens were cut in the vertical plane to a 10 μm thickness on a cryostat, mounted on glass slides and stained with hematoxylin and eosin. The images were obtained using a Leica DMI6000 CS fluorescence microscope, Leica DFC360FX digital video camera and Leica AF6000 software (Laboratory of Applied Biomedical Optics at UNIFESP).

Fluorescence spectral analyses

The blood and feces extracted PPIX solution emission spectra were obtained by exciting the samples at 405 nm using a 1 mm optical path cuvette (Hellma). Sample fluorescence was measured from 550 to 750 nm using a Horiba Jobin Yvon Fluorolog 3 Fluorimeter ((Laboratory of Applied Biomedical Optics at UNIFESP).

Statistical analysis

The data are expressed as the mean ± standard error of the mean (S.E.M.). Statistical comparisons among the groups were performed using a one-way analysis of variance (ANOVA). Probability values of $P < 0.05$ were considered statistically significant. All of the experiments were performed independently and repeated a minimum of three times. The GraphPad Prism 5 package was used.

The effect size,[16] the standardized mean difference between the two groups, was determined by eqn (1):

$$\text{Effect size} = \left[\frac{\text{Mean of EGALA or EGALAAu} - \text{Mean of CG or CGALA}}{\text{Standard deviation}}\right] \quad (1)$$

Standard deviation (pooled)[16] was estimated as an average of the standard deviations of the experimental and control groups and was calculated by eqn (2):

$$\text{SD}_{\text{Spooled}} = \sqrt{\frac{(N_E - 1)\text{SD}_E{}^2 + (N_C - 1)\text{SD}_C{}^2}{N_E + N_C - 2}} \quad (2)$$

where N_E and N_C are the numbers in the experimental and control groups, respectively, and SD_E and SD_C are their standard deviations.

Power analysis was performed using Statistics\Power and Sample Size: PSS_tTest 2 from OriginPro8.

C. Results and discussion

Synthesis and characterization of ALA gold nanoparticles (ALA:AuNPs)

The absorbance of gold colloidal solutions was measured for the solutions prepared with chloroauric acid and polyethylene glycol (PEG). According to the literature, PEGylation leads to a sufficient stability of the material in aqueous media and strong resistance to binding against various biomolecules.[17]

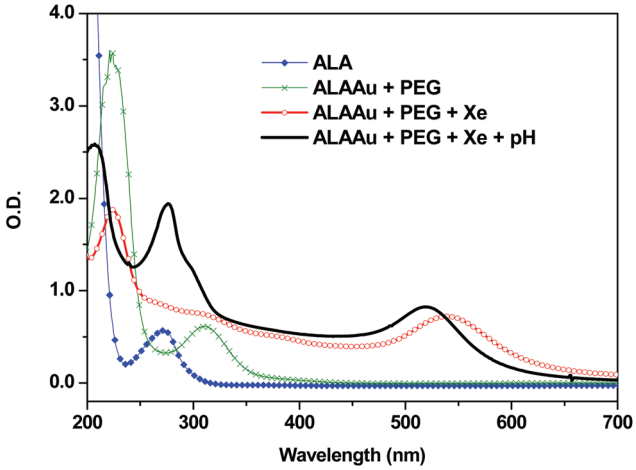

Fig. 1 Optical absorption spectra of gold nanoparticles formed after illumination for 1 minute by a Xe lamp. ALA + PEG ($HAuCl_4$ = 0.02074 g + ALA = 0.08332 g + PEG = 0.02844 g in 200 mL Milli-Q H_2O); ALA + PEG + Xe (ALA + PEG and 2 minutes of Xe light irradiation); ALA + PEG + Xe + pH (ALA + PEG + Xe and pH of the solution adjusted to 7.2).

The results are shown in Fig. 1. Before xenon illumination, an absorption band at approximately 310 nm, characteristic of ALA, is observed. During the Xe light exposure the solution color changes from colorless to purple (Fig. 2a), and after the illumination ends, an absorption peak at approximately 540 nm appears due to the SPR (surface plasmon resonance) effect, indicating the formation of gold nanoparticles.[18] Changing the solution pH from ~3.0 to ~7.0, the absorption peak is blue-shifted and narrowed (Fig. 1), and the solution color becomes reddish (Fig. 2b). The blue shift observed in the spectra can be attributed to the gold nanoparticles' size reduction.

The zeta potential of the solutions was measured, and increasing the solution pH from ~5.0 to ~8.0, a change in its value from ~10 to ~40 mV was observed. Thus, greater stability

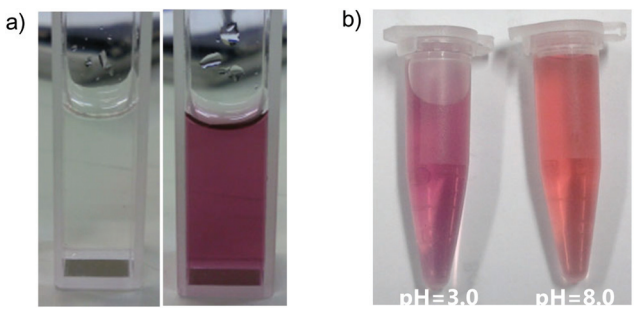

Fig. 2 Color of a gold colloidal suspension: (a) before (left) and after (right) illumination with white light from a Xe lamp for 1 minute and (b) after change in pH from ~3.0 to 7.0.

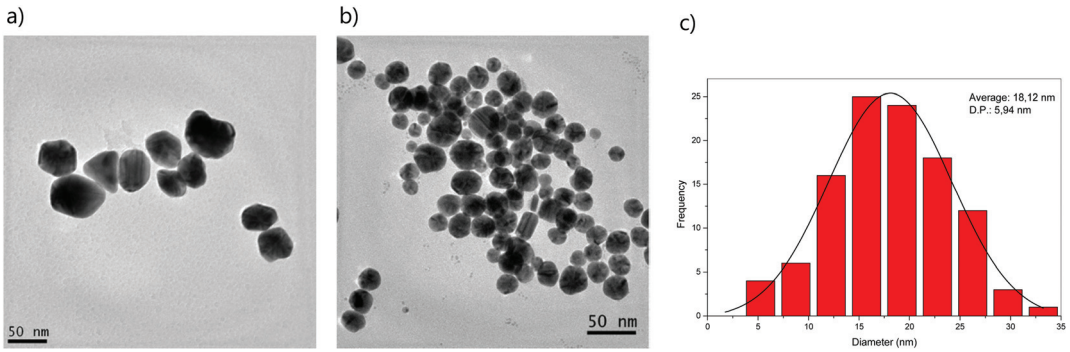

Fig. 3 TEM images of synthesized ALA:AuNPs: (a) ALA + PEG + Xe ($HAuCl_4$ = 0.02074 g + ALA = 0.08332 g + PEG = 0.02844 g in 200 mL Milli-Q H_2O and 2 minutes of Xe light irradiation); (b) ALA + PEG + Xe + pH (ALA + PEG + Xe and pH of solution adjusted to 7.2) and (c) ALA + PEG + Xe + pH size distribution.

is achieved with a basic pH. The increase in pH enables nanoparticles' stabilization against agglomeration and precipitation.

Transmission electron microscopy was used to characterize the size, shape and morphology of the synthesized ALA:AuNPs, and the micrographs of the synthesized particles before and after the pH change are shown in Fig. 3. The ALA:AuNPs after pH correction are nearly spherical with sizes ranging from 5 to 40 nm, as observed in Fig. 3c.

The synthesis of the nanoparticles is possible because light promotes the reduction of gold ions (Au^{3+}) to metallic gold (Au^0) (in an ALA/tetrachloroauric acid solution) and ALA prevents their agglomeration, stabilizing the colloidal suspension.[19] The use of xenon light is important to catalyze this reduction, since ALA by itself does not promote the efficient reduction of gold. The increase in pH recovers the ALA structure, enabling nanoparticle stabilization against agglomeration and precipitation.

ALA:AuNP administration

At baseline, the body weight of all experimental rabbits ranged from 2.2 to 2.4 kg. Over the course of the study, all of the animals gained weight, but no significant difference was observed at any time point. The final weight ranged from 2.4 to 3.4 kg. A comparison of serum lipids in the control and experimental groups (60 days) is shown in Table 2 which shows an increase in the total cholesterol and low density lipoprotein concentrations in the blood with a 1% cholesterol diet. All of the rabbits completed the experimental process.

Previous studies indicate that several types of porphyrins, including PPIX, accumulate in significant amounts in rapidly growing tissues such as atheromatous plaques,[8,15] and in this case the increase in blood PPIX emission follows the growth of the plaques.[20] Since ALA is a precursor in the heme biosynthesis pathway, it is converted to PPIX, which is fluorescent,[21] and through this mechanism it is possible to enhance the PPIX emission present in the blood upon ALA administration.[22] To evaluate the capability of ALA:AuNPs (ALA + PEG + Xe and pH adjusted to 7.2) to convert to PPIX, ALA:AuNPs were orally administered to the animals and porphyrins

Table 2 Serum lipids. Normal control group: rabbits were fed a normal diet; experimental group: rabbits were fed a high-cholesterol-diet for 60 days. Data are presented as the mean ± SEM, n = 4 for the control group and 6 for the experimental group. TC: total cholesterol; HDL-C: high-density lipoprotein cholesterol; LDL-C: low-density lipoprotein cholesterol and glucose

	CG	CG (Er±)	EG (60 days)	EG (Er±)
TC (mg dL^{-1})	76.18	6.82	1344.55	200.13
HDL (mg dL^{-1})	28.34	1.75	23.87	1.94
LDL (mg dL^{-1})	14.56	1.44	558.30	81.26
Glucose (mg dL^{-1})	106.77	8.54	167.87	24.04

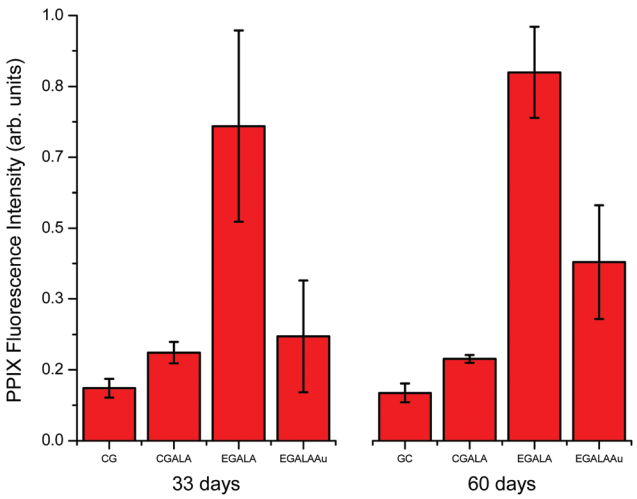

Fig. 4 Differences observed in PPIX fluorescence in blood collected 34 and 60 days after the diet procedure beginning from the control and experimental groups before and after 24 h of ALA and ALA:AuNP administration. Comparing with the control group the two-tailed P values are 0.0228 for 34 days and 0.0005 for 60 days for the ALA group. For the EGALAAu group for 34 days the difference is not considered to be statistically significant and for 60 days the two-tailed P value equals 0.0438.

were extracted from the total blood. PPIX fluorescence was measured and the results are shown in Fig. 4. In this figure, the signal emission area, which was obtained by integrating the endogenous PPIX emission spectra from 550 to 750 nm, is

plotted as a function of the studied groups, control group (CG), control group with ALA (CGALA), experimental group with ALA (EGALA) and experimental group with ALA:AuNPs (EGALAAu). In this case blood was collected 24 hours after ALA or ALA:AuNP administration. Each point corresponds to the average of the signal from each studied group.

The results, shown in Fig. 4, have shown an increase in PPIX fluorescence for animals that received ALA in both the control and experimental groups. The fluorescence intensity increased almost 6.0 fold in the experimental group with ALA in comparison with the control group after 34 days and ~7.7 fold after 60 days. The two-tailed *P* values are 0.0228 for 34 days and 0.0005 for 60 days. By conventional criteria, these differences are considered to be statistically significant. An increase in PPIX fluorescence was also observed after oral ALA:AuNP administration: ~2 fold in the experimental group with ALA in comparison with the control group after 34 days and ~3.7 fold after 60 days. For 34 days the two-tailed *P* value equals 0.3293. By conventional criteria, this difference is not considered to be statistically significant. For 60 days the two-tailed *P* value equals 0.0438. By conventional criteria, this difference is considered to be statistically significant. The sample sizes used in all experiments show an analytical power >0.9, except for 34 days (CGALA × EGALAAu). In this case the number of animals is not sufficient to yield statistical significance (typically 12 animals per group are needed).

The results show that the functionalized gold nanoparticles reached atheromatous plaques and their ALA was converted to PPIX. The selective accumulation of PPIX in plaques provides a contrast between control animals and those with atherosclerosis.

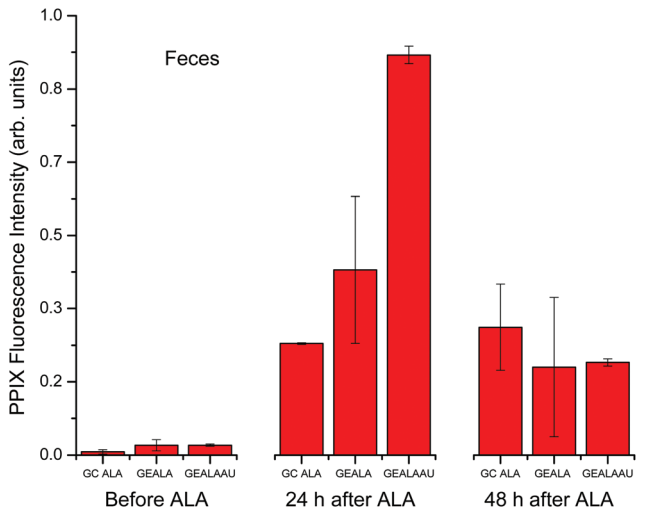

Fig. 5 Differences observed in the coproporphyrin fluorescence in feces collected 33 days after the diet procedure beginning from the control and experimental groups before and after 24 h and 48 h of ALA and ALA:AuNP administration. Considering the data for 24 hours, the two-tailed *P* value found was 0.2856 for EGALA compared with the CGALA group (not significant) and less than 0.0001 for EGALAAu compared with the CGALA group.

The extraction of porphyrin from animal feces (coproporphyrin) collected 33 days after the diet procedure started was also measured and the results are shown in Fig. 5. In this case porphyrin was extracted before, and 24 and 48 h after ALA and ALA:AuNP administration. The results show an increase in porphyrin fluorescence for the three groups after 24 hours, indicating the elimination of porphyrin from the body. Probably the metabolism is faster in the presence of gold nanoparticles. This fact must explain why AuNPs produce an enhanced coproporphyrin fluorescence in feces at 24 h. Comparisons between the averaged intensities for CGALA with EGALA and CGALA with EGALAAu were done. The two-tailed *P* value found was 0.2856 for EGALA and less than 0.0001 for EGALAAu. By conventional criteria, the difference observed for EGALAAu is considered to be extremely statistically significant. In this case the sample size used show an analytical power >0.9. In the comparisons with EGALA the number of animals is not sufficient to yield statistical significance (typically 12 animals per group are needed).

Fig. 6 shows the images obtained from the aortas of the control and experimental groups. As can be observed in

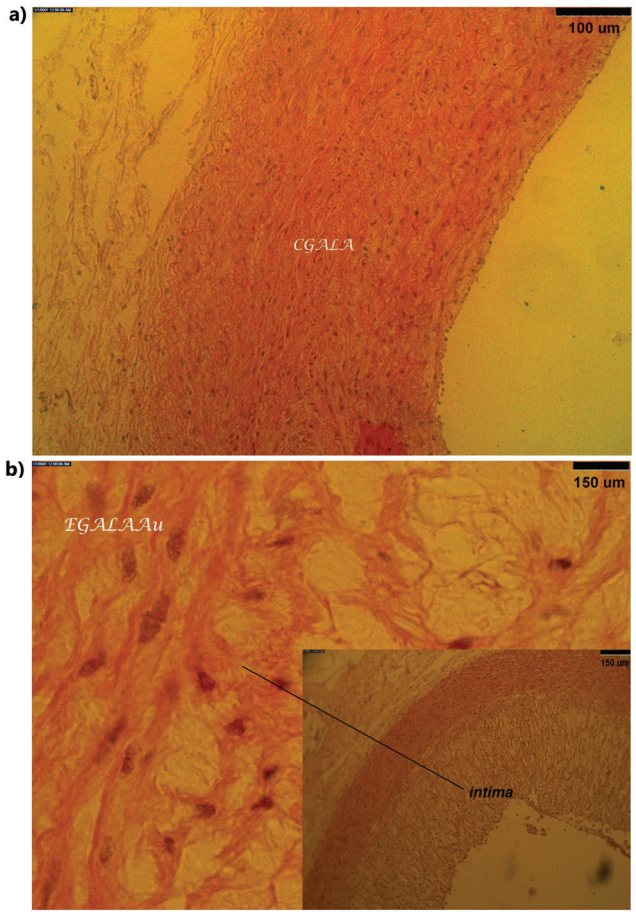

Fig. 6 Microscopic appearance of atherosclerotic lesions of rabbits' aortic arch. (a) Control group. (b) Experimental group (EGALAAuNPs) 100×. The artery shows a thickening of the intima and arterial media. The thickest sections of the arteries show considerable foamy cell infiltration and extracellular lipid accumulation.

Fig. 6a, the aorta of a control group rabbit (normal diet) has normal thickness, and no lipid is present in the intima layer. For experimental group rabbits (high cholesterol diets) the intima layer is thickened (Fig. 6b). All animals from the experimental group presented an increase in the arterial thickness after 60 days (from ~300 to ~900 μm). In Fig. 6b a considerable foamy cell infiltration and extracellular lipid accumulation are seen. No visible alteration was observed due to the presence of gold nanoparticles. Kidneys, lungs and liver tissues also maintain the same aspects for animals from the EGALA and EGALAAu groups.

It is our understanding that this is the first study that analyses porphyrin accumulation in the blood and feces of animals with atherosclerosis after oral ALA:AuNP administration. The PPIX accumulated in atheroma plaques is transferred to blood and feces and can be analyzed by porphyrin extraction. As an excess of heme and PPIX is harmful to the organisms, it needs to be eliminated. In general, the porphyrin fraction of a hemoglobin molecule is released into the blood and later secreted by the liver in bile.[23] However, in atherosclerotic animals, the higher concentration of porphyrin is also excreted by feces.

D. Conclusions

An increase in blood and feces porphyrin emission after ALA:AuNP administration suggests that ALA was incorporated by gold nanoparticles, its structure was preserved, and a rapid conversion into endogenous porphyrins occurred, overloading the synthetic pathway that led to PPIX accumulation. The high accumulation of PPIX in tissues is thought to be the result of uncontrolled cell proliferation that accompanied the growth of atheromatous plaques. This finding indicated that ALA:AuNPs can aid in the early diagnosis and therapy of atherosclerosis with high sensitivity.

Another important characteristic about ALA:AuNPs is their high stability. This fact facilitates drug administration since normally ALA must be freshly prepared and its pH should be adjusted.

The results indicate three clinical approaches for ALA:AuNP administration:

(1) Porphyrin blood and feces screening.

(2) Diagnosis by contrast methods such as computed tomography, magnetic resonance tomography, positron emission tomography, and fluorescence angioscopy. Diagnosis by non-invasive methods such as diffusion reflection is also possible.

(3) Therapy using PDT, sonodynamic or photothermia.

Larger and better designed studies are being developed to elaborate more on this matter, to verify the most appropriate concentration of an ALA:AuNP solution and the best time for its administration in animals.

Acknowledgements

This work was supported by the "Fundação de Amparo a Pesquisa do Estado de São Paulo" (FAPESP), grant number 2010/016544-1. The authors would also like to thank Maira Franco de Andrade for help in veterinary procedures.

References

1 P. Libby, P. M. Ridker and G. K. Hansson, *Nature*, 2011, **473**, 317–325.
2 J. S. Ross, N. E. Stagliano, M. J. Donovan, R. E. Breitbart and G. S. Ginsburg, *Atherosclerosis VI*, 2001, **947**, 271–293.
3 X.-F. Li, C.-Y. Chen, Y.-H. Zhao and X.-Y. Yuan, *Prog. Biochem. Biophys.*, 2014, **41**, 739–748.
4 T. Curry, R. Kopelman, M. Shilo and R. Popovtzer, *Contrast Media Mol. Imaging*, 2014, **9**, 53–61.
5 V. Sanna, N. Pala and M. Sechi, *Int. J. Nanomed.*, 2014, **9**, 467–483.
6 D. Fixler, *SPIE Optical Fibers and Sensors for Medical Diagnostics and Treatment Applications Xiv*, 2014, 8938.
7 J. Xie, S. Lee and X. Chen, *Adv. Drug Delivery Rev.*, 2010, **62**, 1064–1079.
8 C. H. Peng, Y. S. Li, H. J. Liang, J. L. Cheng, Q. S. Li, X. Sun, Z. T. Li, F. P. Wang, Y. Y. Guo, Z. Tian, L. M. Yang, Y. Tian, Z. G. Zhang and W. W. Cao, *J. Photochem. Photobiol., B*, 2011, **102**, 26–31.
9 R. Waksman, P. E. McEwan, T. I. Moore, R. Pakala, F. D. Kolodgie, D. G. Hellinga, R. C. Seabron, S. J. Rychnovsky, J. Vasek, R. W. Scott and R. Virmani, *J. Am. Coll. Cardiol.*, 2008, **52**, 1024–1032.
10 Y. Murayama, Y. Harada, K. Imaizumi, P. Dai, K. Nakano, K. Okamoto, E. Otsuji and T. Takamatsu, *Int. J. Cancer*, 2009, **125**, 2256–2263.
11 M. Benito, V. Martin, M. D. Blanco, J. M. Teijon and C. Gomez, *J. Pharm. Sci.*, 2013, **102**, 2760–2769.
12 C. P. Yao, S. J. Wang, Y. Yang, Y. L. Han, H. Xu, W. H. Zeng and Z. X. Zhang, *Spectrosc. Spectral Anal.*, 2012, **32**, 2519–2522.
13 J. L. Cheng, X. Sun, S. Y. Guo, W. Cao, H. B. Chen, Y. H. Jin, B. Li, Q. N. Li, H. Wang, Z. Wang, Q. Zhou, P. Wang, Z. G. Zhang, W. W. Cao and Y. Tian, *Int. J. Nanomed.*, 2013, **8**, 669–676.
14 F. P. Wang, Q. P. Gao, S. Y. Guo, J. L. Cheng, X. Sun, Q. N. Li, T. Y. Wang, Z. G. Zhang, W. W. Cao and Y. Tian, *Biomed Res. Int.*, 2013, **2013**, 737264.
15 S. Y. Guo, X. Sun, J. L. Cheng, H. B. Xu, J. H. Dan, J. Shen, Q. Zhou, Y. Zhang, L. L. Meng, W. W. Cao and Y. Tian, *Int. J. Nanomed.*, 2013, **8**, 2239–2246.
16 S. Olejnik and J. Algina, *Contemp. Educ. Psychol.*, 2000, **25**, 241–286.
17 C. W. Chung, K. D. Chung, Y. I. Jeong and D. H. Kang, *Int. J. Nanomed.*, 2013, **8**, 809–819.
18 W. Hou and S. B. Cronin, *Adv. Funct. Mater.*, 2013, **23**, 1612–1619.
19 M. Sakamoto, M. Fujistuka and T. Majima, *J. Photochem. Photobiol., C*, 2009, **10**, 33–56.

20 M. N. da Silva, L. B. Sicchieri, F. R. de Oliveira Silva, M. F. Andrade and L. C. Courrol, *Analyst*, 2014, **139**, 1383–1388.
21 L. C. Courrol, F. R. de Oliveira Silva, E. L. Coutinho, M. F. Piccoli, R. D. Mansano, N. D. Vieira Junior, N. Schor and M. H. Bellini, *J. Fluoresc.*, 2007, **17**, 289–292.
22 F. R. de Oliveira Silva, M. H. Bellini, C. T. Nabeshima, N. Schor, N. D. Vieira, Jr. and L. C. Courrol, *Photodiagn. Photodyn. Ther.*, 2011, **8**, 7–13.
23 M. L. Welcker, *N. Engl. J. Med.*, 1945, **232**, 11–19.